Carbon dioxide along WOCE line A14: Water masses characterization and anthropogenic entry

A. F. Ríos, X. A. Álvarez-Salgado, F. F. Pérez, L. S. Bingler, J. Arístegui, Laurent Mémery

Carbon dioxide along WOCE line A14: Water masses characterization and anthropogenic entry

A. F. Ríos,[1] X. A. Álvarez-Salgado,[1] F. F. Pérez,[1] L. S. Bingler,[2] J. Arístegui,[3] and L. Mémery[4]

Received 12 April 2002; revised 31 May 2002; accepted 6 February 2003; published 22 April 2003.

[1] The meridional WOCE line A14, just east of the South Atlantic Mid-Atlantic Ridge, was surveyed during the austral summer of 1995 from 4°N to 45°S. Full-depth profiles of pH, total alkalinity (TA), and total inorganic carbon (C_T) were measured, allowing a test of the internal consistency of the CO_2 system parameters. The correlation between C_T measured and calculated from pH and TA was very good ($r^2 = 0.998$), with an insignificant average difference of 0.1 ± 3.0 μmol kg^{-1} (n = 964 data). CO_2 certified reference materials (CRMs) and a collection of selected samples subsequently analyzed at the Scripps Institution of Oceanography were used to assess the accuracy of our measurements at sea with satisfactory results. The three measured CO_2 system variables were then used to identify the characteristic array of zonal flows throughout the South Atlantic intersected by A14. Equatorial, subequatorial, subtropical, and subantarctic domains were identified at the depth range of the surface water, South Atlantic Central Water (SACW), Antarctic Intermediate Water (AAIW), Upper Circumpolar Water (UCPW), North Atlantic Deep Water (NADW) and Antarctic Bottom Water (AABW). The nonconservative CO_2 system parameters (pH, TA, C_T) have been useful in identifying the transition from aged subequatorial to ventilated subtropical surface, central and intermediate waters. They have been identified as good tracers of the zonal circulation of NADW, with marked flows at the equator, 13°S, and 22°S (the ''Namib Col Current'') and the sharp transition from UNADW to UCPW at 23°S. The anthropogenic CO_2 inventory (C_{ANT}) was estimated and compared with CFC-derived apparent ages for different water masses along A14. The anthropogenic entry reached maximum in the relatively young and ventilated subantarctic and subtropical domains where AAIW was the most efficient CO_2 trap. The calculated annual rate of C_{ANT} entry by AAIW was 0.82 μmol kg^{-1} y^{-1}, in agreement with the annual rate estimated from the equilibrium between the atmospheric pCO_2 increase and the upper mixed layer. *INDEX TERMS:* 4806 Oceanography: Biological and Chemical: Carbon cycling; 4283 Oceanography: General: Water masses; 4223 Oceanography: General: Descriptive and regional oceanography; 4536 Oceanography: Physical: Hydrography; *KEYWORDS:* CO_2, anthropogenic carbon, water masses, South Atlantic

Citation: Ríos, A. F., X. A. Álvarez-Salgado, F. F. Pérez, L. S. Bingler, J. Arístegui, and L. Mémery, Carbon dioxide along WOCE line A14: Water masses characterization and anthropogenic entry, *J. Geophys. Res.*, *108*(C4), 3123, doi:10.1029/2000JC000366, 2003.

1. Introduction

[2] During the last decade, many oceanographers focused their efforts on global ocean circulation in relation to climate. They began the cooperative ''World Ocean Circulation Experiment'' (WOCE) to obtain high-quality hydrographic data complemented with tracer measurements. Since ~30% of the anthropogenic emissions of the greenhouse gas CO_2, seem to have been trapped by the oceans [*Watson et al.*, 1995], knowledge of the CO_2 system parameters, partial pressure (pCO_2), pH, total alkalinity (TA), and total inorganic carbon (C_T), is essential for understanding the regulating action of the ocean on climate. Using the appropriate dissociation constants for carbonic acids [*Millero*, 1995], only two of the four parameters are needed to determine the CO_2 system. Simultaneous measurements of at least one of the remaining two parameters allow a test of the internal consistency. However, field studies including measurements of more than two parameters are scarce [*Millero et al.*, 1993; *Clayton et al.*, 1995; *Lee et al.*, 1997; *McElligott et al.*, 1998; *Johnson et al.*, 1999].

[1]Consejo Superior de Investigacions Cientificas, Instituto de Investigaciones Marinas, Vigo, Spain.
[2]Pacific Northwest National Laboratory, Battelle Marine Sciences Laboratory, Sequim, Washington, USA.
[3]Universidad de las Palmas de Gran Canaria, Las Palmas de Gran Canaria, Spain.
[4]Laboratoire d'Océanographie Dynamique et Climatologie, Institut Pierre Simon Laplace, Paris, France.

0148-0227/03/2000JC000366

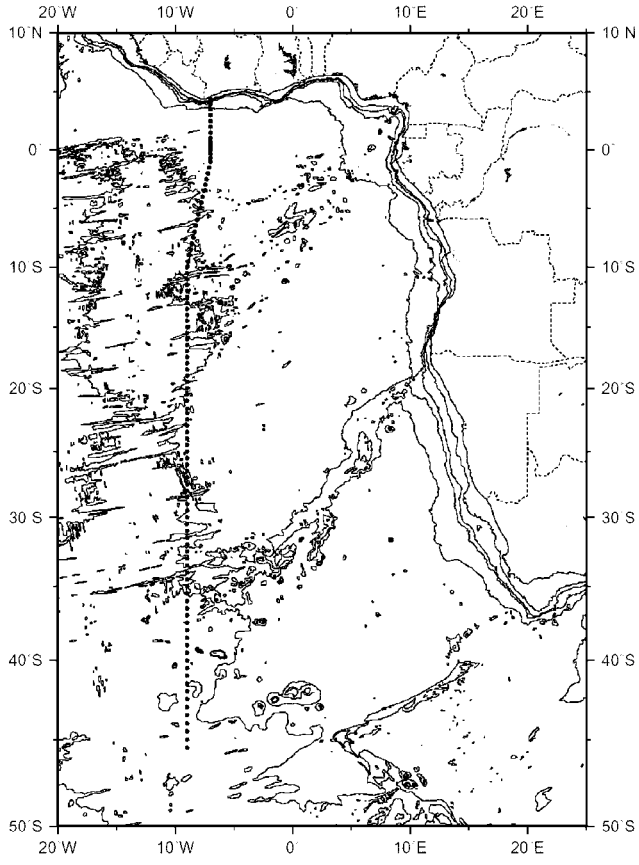

Figure 1. Chart of the eastern South Atlantic Ocean with the position of the 107 full-depth stations surveyed along WOCE line A14. Isobaths 200 m and multiples of 1000 m are reported.

[3] Potentiometric pH and TA and coulometric C_T were measured at sea along WOCE line A14, in the Eastern Equatorial and South Atlantic (Figure 1). CO_2 "certified reference materials" (CRM) were used to test the accuracy of our measurements. In addition, duplicate analyses were performed to examine the precision of these methods. High internal consistency, accuracy, and precision of CO_2 parameters during the cruise allow us to characterize (1) the equatorial, subequatorial, subtropical, and subantarctic regimes imposed by the climatologically driven circulation in the upper ocean [*Peterson and Stramma*, 1991] and (2) the complex advection and mixing of intermediate, deep, and bottom waters of Antarctic origin with deep waters from the north Atlantic that exhibit opposing flow at different depths [*Reid*, 1989; *Peterson and Whitworth*, 1989].

[4] The initial concentrations of the CO_2 parameters in source regions of different water masses are modified by the oxidation of organic materials and the dissolution of carbonaceous skeletons [*Broecker and Peng*, 1982; *Takahashi et al.*, 1985; *Anderson and Sarmiento*, 1994]. In addition, the initial pCO_2, pH, and C_T of any water mass depend on the CO_2 levels in the overlying atmosphere, which have increased from preindustrial reference value of 278 ppm to 359 ppm in 1995 [*Keeling et al.*, 1995]. The total amount of anthropogenic CO_2 dissolved in the ocean can be estimated assuming that (1) dissolved oxygen and CO_2 are close to equilibrium with the atmosphere during water mass formation and (2) alkalinity is not significantly affected by the CO_2 increase [e.g., *Chen and Millero*, 1979; *Poisson and Chen*, 1987; *Gruber et al.*, 1996]. On this basis we have examined the potential of the eastern South Atlantic as a sink for the anthropogenic CO_2 emitted throughout the industrial era. Finally, surface pCO_2 is compared with atmospheric concentration to establish the CO_2 sources and sinks at the time of the cruise in relation to the different zones observed in the upper ocean.

2. Methods

[5] The meridional line A14 was occupied during the first leg of cruise CITHER-3 (R/V L'Atalante, 13 January to 16 February 1995) from 4°N to 45°S along ~9°W (Figure 1). Data from a Neil-Brown Mark IIB CTD probe were acquired from the surface to 15 m above the bottom at 107 sampling stations. Water samples for chemical analyses were collected in 8 liter Niskin bottles at 30 depths throughout the water column. A comprehensive description of the cruise, sampling procedures, analytical techniques, and raw data are given by *Groupe CITHER-3* [1996, 1998]. Data are also available from the WOCE Hydrographic Program Office (http://whpo.ucsd.edu/data/onetime/atlantic/ a14).

2.1. Sample Analyses

[6] Salinity was determined from conductivity measurements with a PORTASAL salinometer using the PSS78 equation [*UNESCO*, 1981] and dissolved oxygen was analyzed by the Winkler method following the recommendations of *Joyce and Corry* [1994]. Oxygen saturation for computing "apparent oxygen utilization" (AOU) was calculated using the equation of Benson and Krause [*UNESCO*, 1986]. Nutrients (nitrate + nitrite, phosphate, and silicate) were analyzed by segmented flow analysis following *Hansen and Grasshoff* [1983], with some modifications [*Mouriño and Fraga*, 1985; *Álvarez-Salgado et al.*, 1992]. Salinity, dissolved oxygen (in μmol kg^{-1}), and nutrients (in μmol kg^{-1}) were determined in all samples collected. Chlorophyll *a* (Chl *a*) concentration in surface samples (in mg m^{-3}) was estimated fluorometrically with a 10,000 R Turner fluorometer after 90% acetone extraction [*Yentsch and Menzel*, 1963]. Chlorofluoromethane CFC11 was measured using an extraction-trapping method in combination with gas chromatography using electron capture detection, as described by *Bullister and Weiss* [1988].

[7] The pH was measured with a Metrohm E-654 pH meter equipped with a Metrohm 6.0233.100 combination glass electrode and a Pt-100 probe for temperature control. The system was standardized with a National Bureau of Standards (NBS) phosphate buffer (pH = 7.413 at 25°C). The Nernstian response of the electrode was tested as described by *Pérez and Fraga* [1987a]. Total alkalinity (TA) was determined by automatic potentiometric titration with HCl ([HCl] = 0.1310) to a final pH of 4.44 [*Pérez and Fraga*, 1987b], using a "Titrino" Metrohm automatic potentiometric titrator with a Metrohm 6.0233.100 combined glass electrode and a Pt-100 probe. The [HCl] was potentiometrically titrated versus borax ($B_4O_7Na \cdot 10H_2O$)

Table 1. The pH_{15}, TA, Measured C_T $(CT)_M$, Calculated C_T $(C_T)_C$ and Calculated pCO_2 on CRMs (Batch 24)[a]

Date	CRMs Analyzed	pH_{15}	TA, $\mu mol\ kg^{-1}$	$(C_T)_M$, $\mu mol\ kg^{-1}$	$(C_T)_C$, $\mu mol\ kg^{-1}$	pCO_2, μatm
17-01-95	5	8.211 (±0.003)	2219 (±1.0)	1988.9 (±1.8)	1987.0 (±1.2)	345 (±3)
17-01-95	4	8.210 (±0.007)	2218 (±0.5)	1985.9 (±1.9)	1986.6 (±3.3)	346 (±6)
19-01-95	5	8.211 (±0.006)	2217 (±0.6)	1986.3 (±0.8)	1984.7 (±2.0)	345 (±5)
20-01-95	4	8.208 (±0.002)	2218 (±0.6)	1986.5 (±1.1)	1987.7 (±0.8)	348 (±2)
21-01-95	4	8.204 (±0.007)	2215 (±2.2)	1986.2 (±0.7)	1987.0 (±2.3)	351 (±5)
22-01-95	4	8.202 (±0.002)	2215 (±0.5)	1987.0 (±0.7)	1988.0 (±0.8)	354 (±2)
24-01-95	7	8.205 (±0.004)	2217 (±0.8)	1986.7 (±1.9)	1988.0 (±1.2)	351 (±4)
25-01-95	4	8.207 (±0.004)	2217 (±0.8)	1986.7 (±1.3)	1987.2 (±1.1)	349 (±4)
27-01-95	5	8.206 (±0.002)	2217 (±1.4)	1985.0 (±1.9)	1987.3 (±1.6)	350 (±2)
28-01-95	4	8.206 (±0.001)	2219 (±1.2)	1986.3 (±2.9)	1989.1 (±1.2)	350 (±1)
31-01-95	5	8.195 (±0.007)	2219 (±0.5)	1986.0 (±2.1)	1994.9 (±2.1)	361 (±4)
31-01-95	1	8.203	2214	1986.2	1986.7	352
2-02-95	4	8.200 (±0.002)	2217 (±0.5)	1984.9 (±3.4)	1990.4 (±2.1)	355 (±5)
4-02-95	5	8.204 (±0.003)	2218 (±1.4)	1984.9 (±1.3)	1989.3 (±1.5)	351 (±3)
6-02-95	4	8.210 (±0.004)	2219 (±1.6)	1985.5 (±0.7)	1987.3 (±2.6)	346 (±4)
9-02-95	8	8.211 (±0.004)	2217 (±1.1)	1986.3 (±1.6)	1985.5 (±1.9)	345 (±3)
10-02-95	3	8.208 (±0.004))	2216 (±0.5)	1986.6 (±3.8)	1986.0 (±2.4)	348 (±4)
Average		8.206 (±0.004)	2217.2 (±1.4)	1986.2 (±0.9)	1987.8 (±2.2)	350 (±4)
CRM	Batch 24	8.205[b]	2216.0 (±1.0)	1987.55 (±1.3)		350.7[c]

[a]Standard deviation of the CRMs analyzed per day (2nd column), in brackets. The pCO_2 was calculated using pH_{15} and TA.
[b]The pH(NBS) calculated from C_T and TA of CRM at 15°C. Independent measurements of pH(SWS) at 25°C were performed on CRMs and converted to the NBS scale at 15°C (pH_{15} = 8.203) using the activity coefficient of *Mehrbach et al.* [1973].
[c]The pCO_2 was calculated from certified C_T and TA at 15°C.

to a final pH of 5.3 ± 0.05 [*Pérez and Fraga*, 1987b]. The pHs were measured at lab temperature and referred to 15°C (pH_{15}) using the parameterisation of *Pérez and Fraga* [1987a], and TA results are expressed in $\mu mol\ kg^{-1}$. Full water column profiles of pH_{15} were produced at each of 107 stations occupied, whereas TA was determined at 39 stations. Additionally, TA of the surface sample was measured at each station.

[8] C_T samples were collected following the procedure described by *U.S. Department of Energy* [1994] and preserved immediately with a saturated mercuric chloride solution to prevent biological production or consumption of CO_2. Samples were analyzed within 14 h after collection; in the meantime they were kept cool and in the dark. The C_T concentration was measured using a ''Single Operator Multiparameter Metabolic Analyzer'' (SOMMA) [*Johnson et al.*, 1987, 1993] coupled with coulometric detection. The seawater sample was drawn into a calibrated pipette and dispensed into a stripping chamber, where it was acidified with 8.5% phosphoric acid. The resultant CO_2 was carried into a coulometric cell with high purity N_2 gas (99.95%) where it was absorbed by and reacted with ethanolamine in dimethylsulfoxide. Seawater samples were collected at 42 stations to provide full C_T profiles. Samples from the upper 1000 m were analyzed at 11 additional stations, to provide C_T data in the main thermocline. C_T and TA have been normalized to salinity 35.0 to produce the corresponding NC_T and NTA parameters.

2.2. Precision, Accuracy, and Internal Consistency of Measured CO_2 Parameters

[9] At least one pair of Niskin bottles were closed at the same depth at each sampling station (field duplicate), providing a check of shipboard methodology precision. The average absolute difference between duplicate analyses was 0.003 for pH_{15} and 1.1 $\mu mol\ kg^{-1}$ for TA, based on 174 and 61 field duplicates, respectively. In addition, each of 30 bottles of the rosette sampler were closed at ~3000 m depth at station 45. The standard deviation of the 30 analyses of pH_{15} and TA were 0.002 and 0.7 $\mu mol\ kg^{-1}$, respectively. Analyses of C_T field duplicates were performed ten times, with an average absolute difference of just 0.3 $\mu mol\ kg^{-1}$. The average absolute difference of 80 laboratory duplicate C_T analyses was 0.8 $\mu mol\ kg^{-1}$. These laboratory analyses were performed by R. F. Keeling at Scripps Institution of Oceanography (SIO) immediately following the cruise.

[10] The accuracy of the measured CO_2 parameters was tested by means of ''Certified Reference Materials'' (CRMs) supplied by A. G. Dickson (University of California). CRMs (batch 24) were analyzed routinely every twenty samples for a total of 114 C_T measurements. The average difference from the certified C_T value (1987.55 $\mu mol\ kg^{-1}$) was <0.94 $\mu mol\ kg^{-1}$. The pH_{15} and TA were also measured routinely using CRMs (Table 1). The average of 76 CRM analyses for TA (2217.2 ± 1.4 $\mu mol\ kg^{-1}$) was in very good agreement with the certified concentration (2216.0 ± 1.0 $\mu mol\ kg^{-1}$). In addition, ten selected C_T samples were collected at seven stations along the cruise to be analyzed by P. Guenther (SIO) by the manometric method (Table 2). The results reinforce the accuracy of shipboard C_T measurements, with 0.9 ± 2.4 $\mu mol\ kg^{-1}$ as the average difference between samples analyzed at SIO and those analyzed on the ship.

[11] C_T was calculated from pH_{15} and TA using the thermodynamic equations of the carbonate system [*Dickson*, 1981] with the dissociation constants of *Mehrbach et al.* [1973], the pK_B of *Lyman* [1956] recalculated by *Edmond and Gieskes* [1970], and K_W of *Dickson and Riley* [1979]. Analytical errors of ±0.003 in pH and ±1.1 $\mu mol\ kg^{-1}$ in TA produce errors of ±1.2 and ±1.1 $\mu mol\ kg^{-1}$ in C_T, estimated from the thermodynamic equations and the average values of pH_{15}, TA, salinity, and temperature during the cruise. Consequently, the total error from the calculation of C_T is

Table 2. Comparison of C_T Measurements Performed by the Coulometric Method on Board and the Manometric Method at the Scripps Institution of Oceanography (SIO) at Ten Selected Samples[a]

Station	Bottle	$(C_T)_M$	$(C_T)_C$	$(C_T)_{SIO}$	$(C_T)_{SIO}-(C_T)_M$	$(C_T)_{SIO}-(C_T)_C$
10	32	1906.7	1903.7	1910.0	3.4	6.4
22	32	2015.6	2015.6	2017.9	2.3	2.3
22	14	2188.9	2188.4	2189.8	0.8	1.3
49	22	2078.9	2077.1	2078.8	−0.1	1.7
49	4	2199.0	2202.1	2199.5	0.5	−2.6
55	32	2078.0	2075.5	2073.7	−4.2	−1.8
55	10	2199.2	2200.0	2197.3	−1.9	−2.8
76	31	2052.6	2056.0	2056.6	4.0	0.5
88	31	2041.6	2041.9	2043.8	2.3	1.9
100	31	2058.9	2059.0	2060.7	1.9	1.7
Average difference					0.9	0.9
Standard deviation					2.4	2.6

[a]C_T calculated from pH and TA measurements on board are included as well. $(C_T)_M$ and C_T are measured coulometrically, $(C_T)_C$ and C_T are calculated from pH_{15}-TA, and $(C_T)_{SIO}$ and C_T are measured manometrically at SIO. Concentrations in μmol kg^{-1}.

±2.3 μmol kg^{-1}. The regression between measured and calculated C_T was very high (Figure 2). The average difference between calculated and measured C_T during the cruise was 0.1 μmol kg^{-1}, with an average error of the $(C_T)_M$ estimate of ±3 μmol kg^{-1}. Finally, calculated C_T for 76 CRMs (Table 1) agrees well with the certified concentration and the average difference of the 10 C_T samples measured at SIO and calculated from pH_{15} and TA (Table 2) was only 0.9 ± 2.6 μmol kg^{-1}. The results of these comparisons prove the high internal consistency of our data. Consequently, good precision, accuracy, and internal consistency of shipboard CO_2 measurements along line A14 make our data reliable for carbon studies in the South Atlantic.

[12] Surface pCO_2 can be calculated from $pH_{15}-TA$, $pH_{15}-C_T$, and $TA-C_T$ using the thermodynamic equations of the carbonate system and the acid constants described above, together with the solubility coefficient of CO_2 in seawater [*Weiss*, 1974]. Analytical errors of ±0.003 in pH_{15}, ±1.1 μmol kg^{-1} in TA, and ±0.8 μmol kg^{-1} in C_T produced errors of ±3.5, ±0.2 and ±2 μatm in pCO_2, respectively. The resultant total errors for the $pH_{15}-TA$, C_T-TA, and $pH_{15}-C_T$ pairs were ±3.7, ±5.5, and ±2.2 μatm, respectively. Correlation between these three sets of calculated pCO_2 values was very high ($r^2 > 0.98$) and the average difference was within the error of the pCO_2 estimate. For this study then, we have used the average of three estimates of surface pCO_2. Calculated pCO_2 of CRMs from $pH_{15}-TA$ (Table 1) had an average standard deviation of ±4.0 μatm, in agreement with the expected error of the pCO_2 estimate.

3. Results and Discussion

3.1. Imprint of the Eastern South Atlantic Circulation on Carbon System Variables

[13] A14 is the westernmost WOCE line in the eastern South Atlantic. It is situated just east of the Mid Atlantic Ridge (Figure 1) and affected by the well-defined zonal circulation of the South Atlantic Ocean [*Peterson and Stramma*, 1991]. The objective of this part is the identification of the main zonal regimes (equatorial, subequatorial, subtropical, and subantarctic) at the level of surface, central, intermediate, and deep waters along line A14, by means of measured and derived CO_2 system variables. The effect of this zonation on the entry of anthropogenic carbon will be assessed in section 3.2.

3.1.1. Upper Ocean

[14] The climatologically driven upper ocean circulation originates a marked zonal array on thermocline waters, which produces a clear impact on the thermohaline and CO_2 system distributions (Figures 3, 4, 5, and 6). The 13°C isotherm, superimposed on the salinity distribution (Figure 3), was used to delimit the different zonal regimes observed along line A14 [*Brea*, 1998]. This isotherm is well within the South Atlantic Central Water (SACW) domain, which ranges from 10°C to 18°C [*Gordon and Bosley*, 1991].

[15] From north to south, line A14 began at 4°N (Figure 3). In the Equatorial Current System (ECS), between 4°N and 3°S, the 13°C isotherm was situated at ∼250 m depth. Poleward rising to 100 m was observed near 3–4°S, which marks the eastward flowing South Equatorial Under-Current (SEUC) at the boundary between the ECS and the Sub-

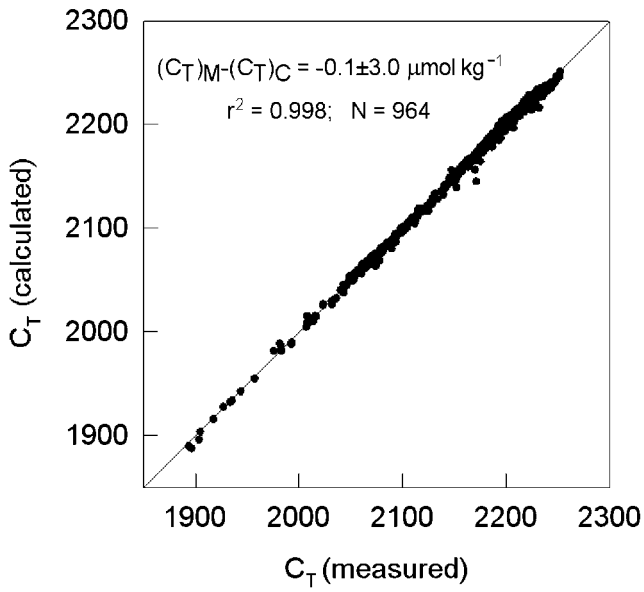

Figure 2. Relationship between C_T calculated and C_T measured. The 1:1 line and the regression equation are reported.

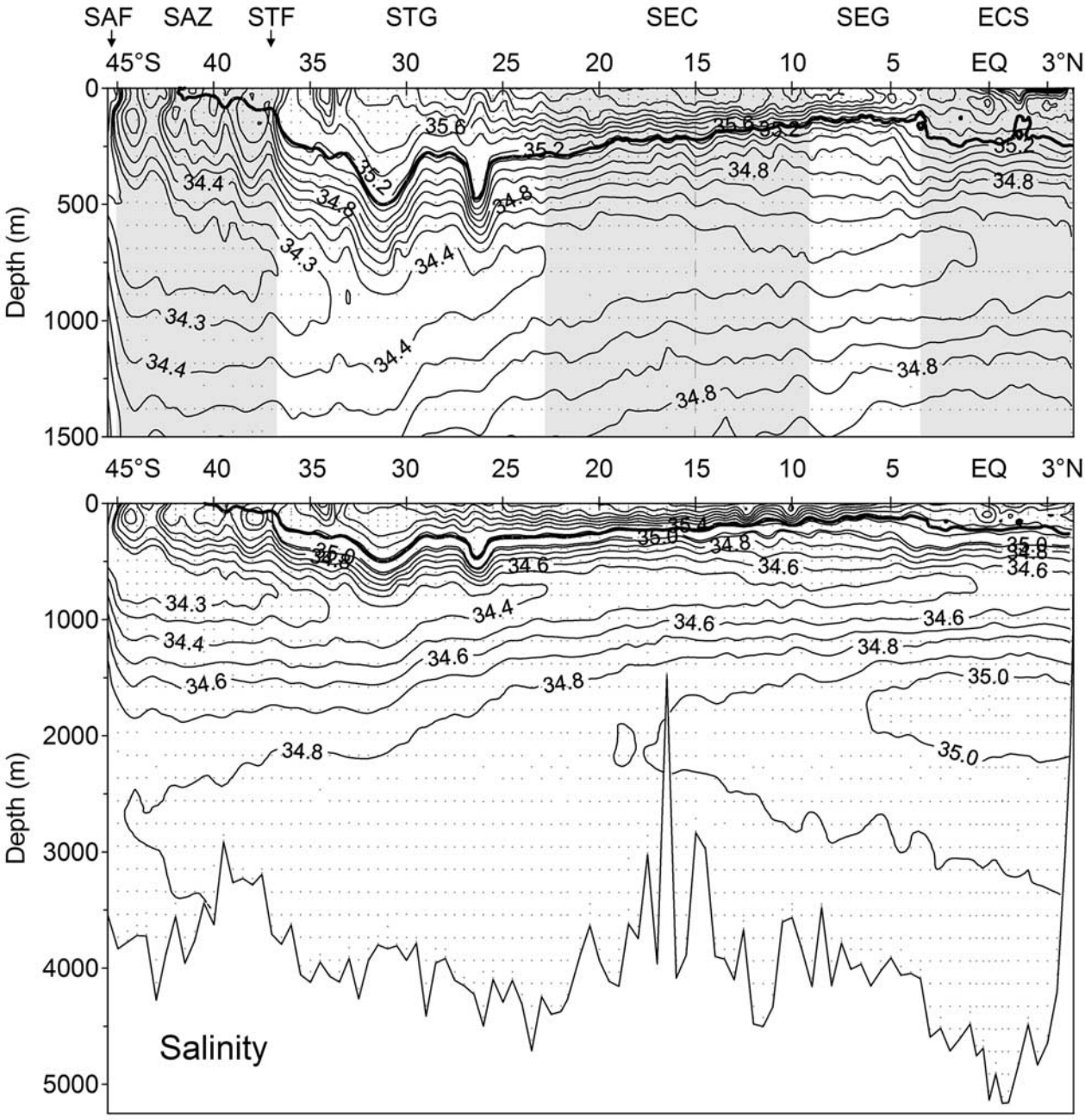

Figure 3. Vertical distribution of salinity along line A14. The 13°C isotherm is depicted. ECS is Equatorial Current System, SEG is South Equatorial Gyre, SEC is South Equatorial Current, STG is Subtropical Gyre, STF is Subtropical Front, SAZ is Subantarctic zone, and SAF is Subantarctic Front. Vertical dashed line represents subtropical-subequatorial transition.

equatorial Gyre (SEG). The 13°C isotherm was present at 125–150 m in the SEG domain (4–9°S). Poleward deepening was observed from 9°S to 23°S, tracing the northwest flowing South Equatorial Current (SEC). The 13° isotherm reached 300 m depth at 23°S. In the Subtropical Gyre (STG), between 23°S and 36°S, the isotherm was found at ~325 m. Two V-shaped structures deepening about 200 m were evident at 26°S (stations 68–69) and 31.5°S (stations 77–79) that correspond with two eddies detached from the Agulhas current [*Arhan et al.*, 1999]. At 36–37°S the 13°C isotherm rose abruptly from 250 to 100 m, denoting the Subtropical Front (STF). Further south, within the Subantarctic Zone, the isotherm rose to shallower depths (~40 m) and disappeared south of 41°S.

3.1.1.1. Surface Waters

[16] Surface distributions of temperature, salinity, chlorophyll, and pCO_2 (Figure 7) are very sensitive to the observed zonal regimes. Therefore it is the objective of this section to study how the contemporary uptake of atmospheric CO_2 in the Eastern South Atlantic was affected by

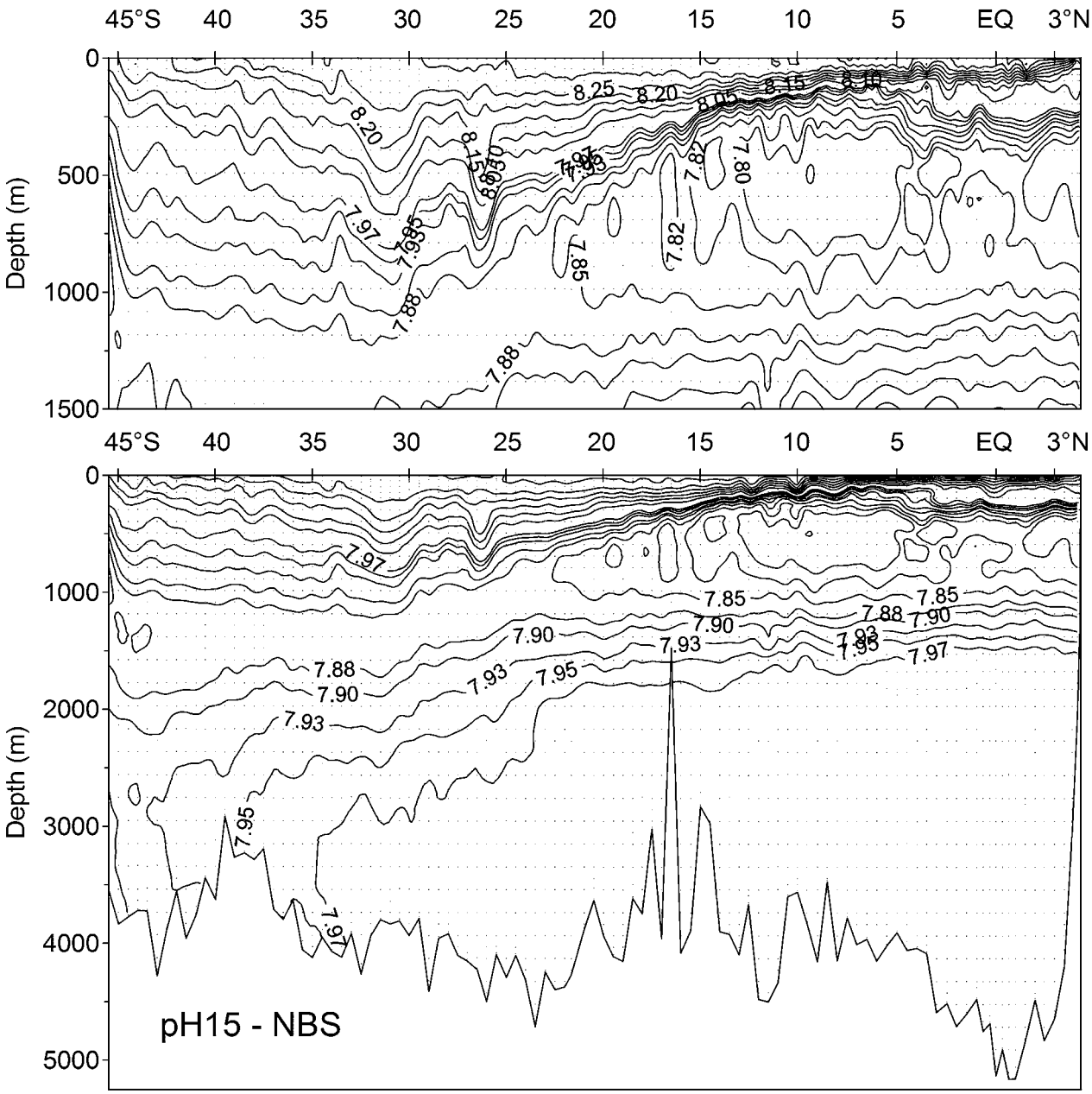

Figure 4. Vertical distribution of pH_{15} along the line A14.

such zonal arrangement. The average mole fraction in dry air of CO_2 (xCO_2) for 1995, 359 ppm according to *Keeling et al.* [1995], is represented by the dotted line in Figure 7b.

[17] Surface waters were pCO_2 undersaturated north of the Equator, reaching a minimum of 313 μatm at 4°16′N, where maximum surface chlorophyll *a* was recorded (3 mg m^{-3}). An area of constant surface pCO_2 (~330 μatm) and very low chlorophyll concentrations (~0.08 mg m^{-3}) appeared just south of the pCO_2 minimum (Figure 7b) and extended up to 2°N. In this zone, nutrients were depleted at the surface and the nutricline was located at ~20 m (not shown). Maximum surface temperature were recorded (>28°C) when salinity was <35 (Figure 7a). The salinity minimum and temperature maximum in this region is known as the Low-Salinity Region (LSR) and is expected to be pCO_2 undersaturated [*Bakker et al.*, 1999]. The position of the LSR corresponds to the Intertropical Convergence Zone (ITCZ), where the wind systems of the two hemispheres converge producing high precipitation, lower salinity, and higher sea surface temperature. The position of this zone varies seasonally, being close to the equator in winter and moving northward in summer [*Siedler et al.*, 1992]. Similar results of low salinity accompanied by low pCO_2 were found during several cruises executed in different seasons, suggesting that the LSR is a recurring or possibly a permanent feature [*Oudot and Andrié*, 1989; *Lefèvre et al.*, 1998; *Bakker et al.*, 1999]. Surface salinity and temperature at the LSR along A14 were 1 unit lower and 6°C higher than at 20 m depth, where pCO_2 levels rose to 485 μatm. Therefore the contribution of CO_2-free rain-

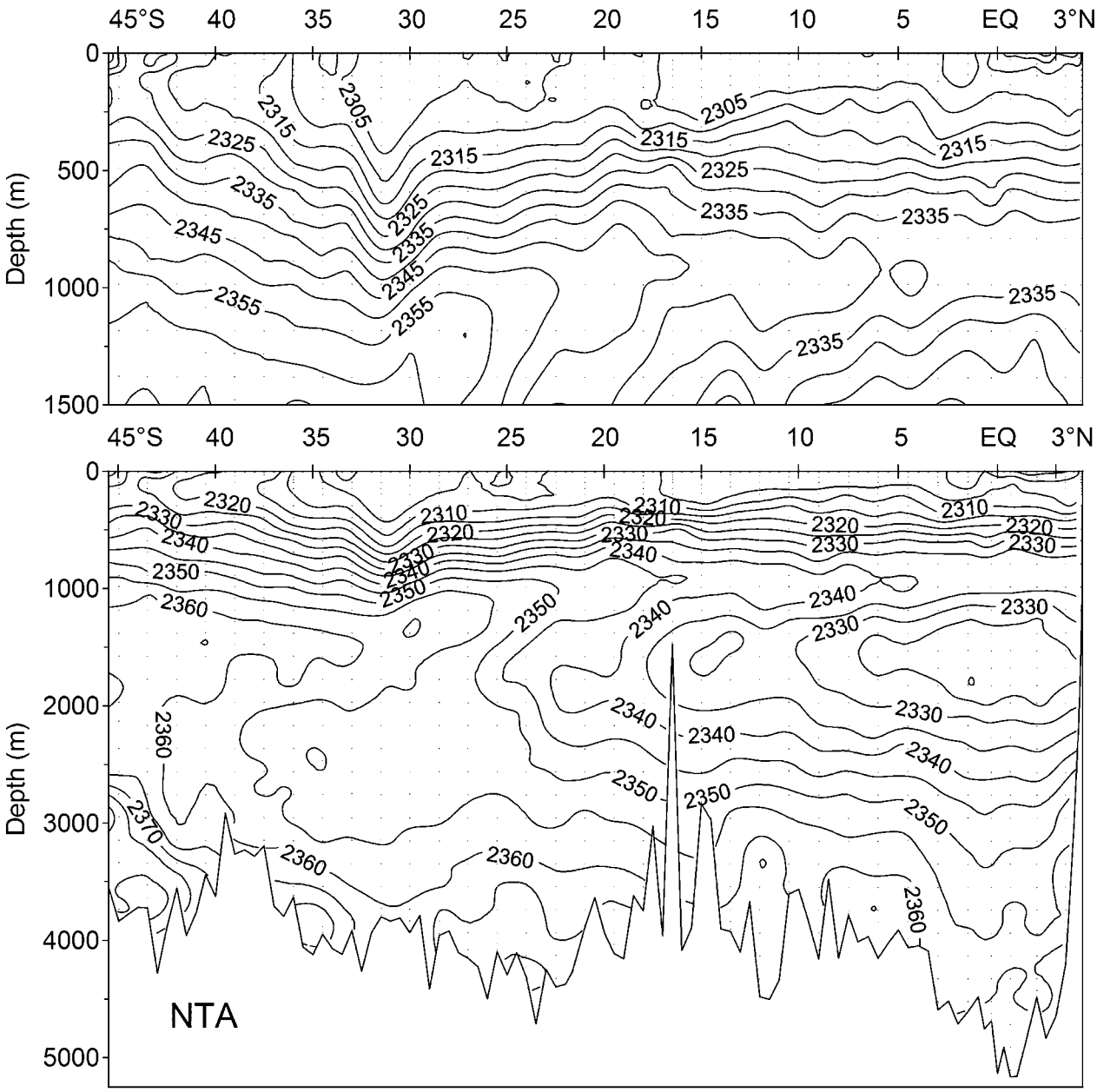

Figure 5. Vertical distribution of normalized total alkalinity (NTA) in μmol kg^{-1} along line A14. Dotted line represents meridional evolution of the UCPW NTA maximum.

water to the composition of surface waters in the LSR was about 3% compared with seawater at 20 m depth. This dilution produces a decrease of 65.8 μmol kg^{-1} in TA and a corresponding pCO_2 decrease of 14 μatm (from 485 to 471 μatm). Since surface pCO_2 in the LSR decreases to 330 μatm, intense net primary production must be the cause of the observed low-surface pCO_2. This seems contradictory because chlorophyll concentrations in the LSR were quite low. However, it must be noted that (1) surface pCO_2 does not depend only on surface chlorophyll but on its vertical distribution and (2) chlorophyll is not an index of primary production but an index of the biomass retained in the water column after grazing and sedimentation of primary producers. The fact that pH in surface waters was 0.24 units higher than at the nutricline suggests intense net primary production in the LSR. This pH increase resulted in a pCO_2 decrease of 294 μatm (from 485 to 191 μatm). The difference between the observed (330 μatm) and the expected (485 − 14 − 294 = 177 μatm) surface pCO_2 levels after consideration of freshwater dilution and net primary production (330 − 177 = 153 μatm) was due to the surface temperature increase of 6°C. Therefore the combination of thermohaline characteristics and biological activity can explain the low pCO_2 values in the LSR at the time of A14 (January–February 1995).

[18] In the 0–4°S zone, salinity increased abruptly and temperature decreased slowly (Figure 7a), due to equatorial upwelling. Surface pCO_2 also increased, reaching values near

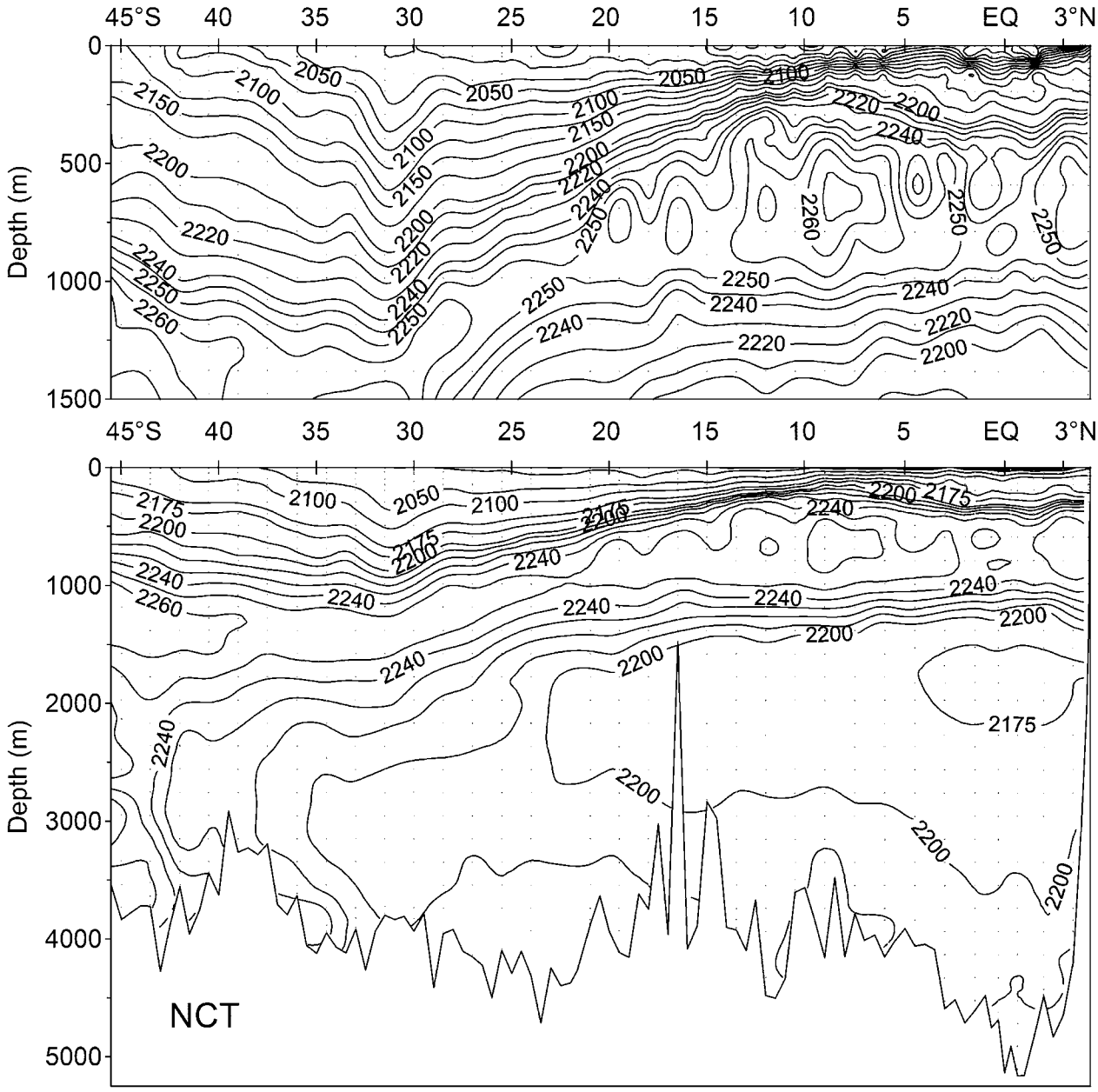

Figure 6. Vertical distribution of normalized total inorganic carbon (NC_T) in μmol kg^{-1} along line A14. Dashed line represents equatorial/subequatorial SACW NC_T maximum. Dotted line represents meridional evolution of the UCPW NC_T maximum.

400 μatm, whereas chlorophyll levels were ~0.15 mg m^{-3} (Figure 7b). Despite low surface pCO_2 levels in the LSR, the whole equatorial zone (4°N–4°S) was pCO_2 oversaturated acting as a CO_2 source to the atmosphere. The average ± std oversaturation (ΔpCO_2) for the whole equatorial zone was 9 ± 29 μatm at the time of A14. *Andrié et al.* [1986] and *Smethie et al.* [1985] obtained similar values (8 ± 19 μatm and 11 ± 17 μatm, respectively) at the same time of the year (January–February) farther east. The extremely high ΔpCO_2 (45 ± 25 μatm) recorded by *Oudot et al.* [1987] was attributed to a climate condition anomaly in 1984.

[19] Surface salinity increased while temperature decreased along the SEG zone (4–9°S), where pCO_2 values were constant (402 ± 5 μatm) and chlorophyll decreased from 0.15 to 0.03 mg m^{-3}. The highest salinity values (36.5 ± 0.1) were observed in the SEC zone (9–23°S) in combination with relatively low temperatures (24.6 ± 0.6 °C). The conspicuous V-shaped pCO_2 distribution centered at ~13°S traced the limit between the subtropical and subequatorial regimes. A local chlorophyll maximum (0.36 mg m^{-3}) was observed at that position, coinciding with local pCO_2 minimum (383 μatm). Temperature decrease and net primary production could be the causes of these relatively low pCO_2 values. It should be noted that the depth of the nutricline at the center of the SEC was located at 137 m, while in the equatorial zone it was found at 20 m depth.

[20] Within the STG salinity, temperature, and pCO_2 decreased by 1.3, 1.3°C and 75 μatm, respectively, from

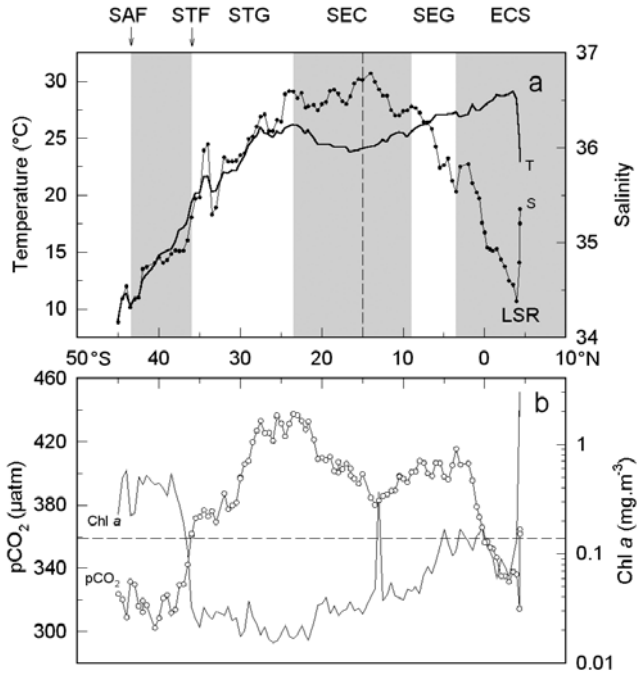

Figure 7. Distribution of (a) surface salinity and temperature (°C) and (b) surface pCO_2 (µatm) and chlorophyll a (mg m^{-3}) along the line A14. ECS is Equatorial Current System, SEG is South Equatorial Gyre, SEC is South Equatorial Current, STG is Subtropical Gyre, STF is Subtropical Front, SAZ is Subantarctic zone, and SAF is Subantarctic Front. Vertical dashed line in Figure 7a represents subtropical/subequatorial transition. Horizontal dashed line represents the mole fraction in dry air (xCO_2) for 1995 (359 ppm) according to *Keeling et al.* [1995].

23°S to 36°S. Chlorophyll concentrations were constant below the detection limit (~0.03 mg m^{-3}). South of the STF (36–37°S) a sharp decrease of surface pCO_2 levels was observed, reaching values below saturation. The pCO_2 undersaturation was caused by low temperatures associated with Subantarctic Surface Water and increased biological activity in the Subantarctic Zone, which produced high surface chlorophyll concentrations of ~0.4 mg m^{-3}. Net primary production was favored in the Subantarctic Zone by a marked increase of surface nutrient concentrations; nitrate reached >15 µmol kg^{-1} in the southern end of A14 at the SAF (not shown). Although surface salinity in the Subantarctic and Equatorial zones was quite similar, TA clearly indicates the difference in origin of surface waters in these two regions. The TA-S plot shows two well-defined ($r^2 > 0.99$) linear relationships north and south of 33°S (Figure 8). For any salinity <36, TA was greater to the south (Subantarctic Surface Water influence) than to the north (Equatorial LSR influence).

[21] More than 80% of the total variability of surface pCO_2 along A14 can be explained by a multiple linear regression with surface salinity and temperature ($r^2 = 0.81$, n = 107; $p < 0.001$). The remaining 20% have to be due to the local effect of net primary production. In fact, a significant negative correlation was observed between surface pCO_2 and chlorophyll ($r^2 = 0.21$, n = 106, $p < 0.001$).

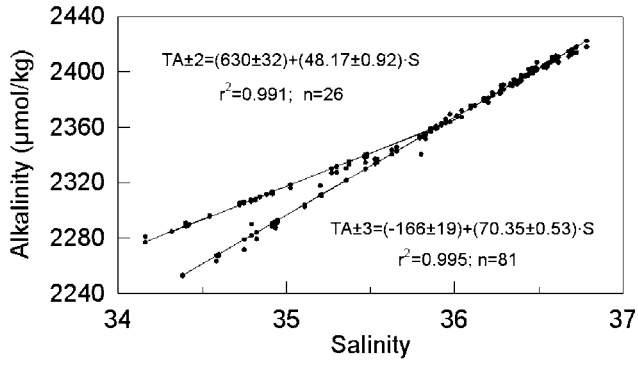

Figure 8. Relationship between total alkalinity (µmol kg^{-1}) and salinity in surface waters along line A14. The corresponding linear regressions are reported.

However, the multiple regression of surface pCO_2 with salinity, temperature, and chlorophyll did not significantly improve the regression with the thermohaline properties ($r^2 = 0.82$, n = 106, $p < 0.001$) due to the inadequacy of chlorophyll measurements to represent net primary production.

3.1.1.2. Central Waters

[22] The evolution of salinity and CO_2 system variables (pH_{15}, NC_T, and NTA) along the 13°C isotherm (Figure 9) clearly show the effect of different zonal regimes in the SACW domain. Salinity remained constant at 35.29 ± 0.01 north of 15°S where a sharp decrease of 0.13 was observed, denoting the abrupt transition from the subequatorial to the subtropical SACW branches. The observed salinity excess of subequatorial SACW on the eastern South Atlantic could be due to regional excess evaporation in the SEG [*Gordon and Bosley*, 1991] or transport of the Salinity Maximum Water formed in the tropical western South Atlantic by the

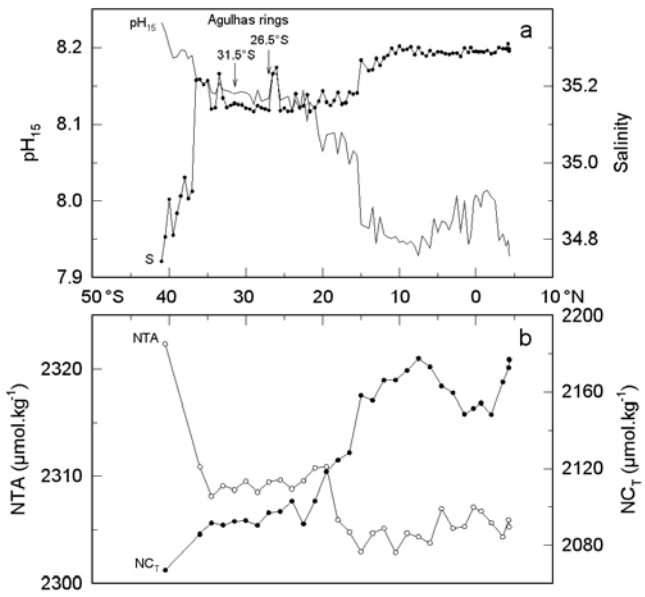

Figure 9. Meridional evolution of (a) salinity and pH_{15} and (b) NC_T and NTA in µmol kg^{-1} along the SACW 13°C isotherm.

SECC [*Mémery et al.*, 2000]. Salinity along the 13°C isotherm was constant at ~35.16 from 15°S to the STF (36–37°S). South of the STF, salinity decreased abruptly coinciding with a sudden rise of the 13°C isotherm in the subantarctic zone.

[23] The pH_{15} levels along the 13°C isotherm increased southwards. The most conspicuous features were a local maximum (excess of ~0.05 units) between 3°N and 3°S and successive steep increases of ~0.10 units at 15°S (subequatorial-subtropical transition) and ~0.05 units at 21–22°S (northern limb of the STG) and at 36–37°S (STF). Maximum pH_{15} values (8.23) were recorded within the Subantarctic Zone, coinciding with an observed salinity minimum. The evolution of NC_T was opposite that of pH_{15} (Figure 9b), with an excess of ~60 μmol kg^{-1} in the SEG compared to the STG as a result of a sudden NC_T change between 15°S and 23°S. On the other hand, NTA concentrations showed a brief excess of ~4 μmol kg^{-1} in the subtropical SACW domain. The observed $\Delta NC_T/\Delta NTA$ molar ratio of −15 between SACW at 13°C in the SEG and the STG indicates that >96% of the NC_T excess in the SEG results from organic carbon oxidation rather than from $CaCO_3$ dissolution, as expected at these shallow levels (140 m). It should be noted that the NC_T excess in the SEG is maximum at 400–700 m depth, where extreme pH_{15} and NC_T values of <7.80 and >2265 μmol kg^{-1} were recorded (Figures 4 and 6). The low pH_{15} and high NC_T concentrations observed were due to the sedimentation associated with high net primary production rates in the surface water [*Reid*, 1989] and prolonged residence time (4.4 and 8.5 years) of thermocline waters in the SEG [*Gordon and Bosley*, 1991].

[24] The Agulhas ring centered at 26°S clearly affected salinity and pH_{15} distributions along the 13°C isotherm (Figure 9a). The pH_{15} values were 0.03 units higher than in the surrounding waters. Expected NC_T and NTA minima were not observed (Figure 9b) because these variables were not measured at stations where the 26°S ring was located. On the contrary, although the 31.5°S ring was sampled, no indications of its presence appeared in any of the plotted distributions. According to *Arhan et al.* [1999], the 26°S ring remained at the higher latitudes of the Agulhas retroflection region during a winter, where it experienced a large heat loss (it is 3.5°C cooler than the second ring) and ventilation, causing an increase of oxygen (13 μmol kg^{-1} higher than the ring centered at 31.5°S). This resulted in a net increase of pH_{15} and therefore an expected decrease of NC_T.

3.1.2. Intermediate and Deep Waters

[25] Below the thermocline, carbon-rich waters of Antarctic origin mix with carbon-poor waters of North Atlantic origin. The northward spread of Antarctic Intermediate Water (AAIW) in the South Atlantic has been traditionally marked by a conspicuous salinity minimum clearly observed in Figure 3 [e.g., *Wüst*, 1935; *Reid*, 1989]. The meridional evolution of the AAIW salinity minimum denotes the sequence of zonal regimes observed in thermocline waters, as previously described in great detail by other authors [*Warner and Weiss*, 1992; *Boebel et al.*, 1997]. We note here a sudden pH_{15}, NTA, and NC_T changes at the level of the AAIW salinity minimum (not shown) denoting the transition from the ventilated subtropical to the aged subequatorial AAIW domains that occurred at 23°S, i.e., 7° south of the transition in the overlying SACW domain.

[26] The northward spread of the aged Upper Circumpolar Water (UCPW) can be traced by the meridional evolution of the NTA and NC_T maxima (Figures 4, 5, and 6) observed just below the AAIW salinity minimum at the southern end of A14. UCPW was present at ~1400 m from the SAF to the STF with NTA and NC_T concentrations of 2364 and 2265 μmol kg^{-1}, respectively. Equatorward rising of these extrema occurred throughout the STG up to ~1000 m at 23°S, where NTA and NC_T concentrations were 2350 and 2250 μmol kg^{-1}, respectively. North of 23°S the NTA and NC_T extrema did not occur at the same depth. The NC_T maximum coincided with the AAIW salinity minimum centered at 800 m. The NTA maximum (~2342 μmol kg^{-1}) remained at 1000 m, coinciding with the silicate maximum (~34 μmol kg^{-1}) and the CFCs minimum (~0.01 pmol kg^{-1}) in the subequatorial and equatorial domains (not shown). The presence of appreciable volumes of UCPW north of the subtropical-subequatorial transition is still a matter of open discussion. *McCartney* [1993], *Andrié et al.* [1998], and *Oudot et al.* [1998] identified the property extrema at 1000 m depth as UCPW. Conversely, *Tsuchiya et al.* [1994] considered that they are really part of the AAIW domain, and *Larqué et al.* [1997] suggested that the UCPW progresses northward to about 24°S in the western basin and most of it returns southwards in the eastern basin. As a consequence of this controversy, *Stramma and England* [1999] give no circulation scheme in the most recent review of the South Atlantic circulation.

[27] The Deep Western Boundary Current (DWBC) transports North Atlantic Deep Water (NADW) from the Northern Hemisphere into the South Atlantic. Frequently, the NADW is separated into three layers: upper, middle, and lower NADW [e.g., *Wüst*, 1935; *Friedrichs et al.*, 1994; *Stramma and England*, 1999]. UNADW along A14 can be clearly distinguished by extreme values of all parameters ($S > 35$, $pH_{15} > 7.99$, NTA < 2325 μmol kg^{-1}, $NC_T < 2190$ μmol kg^{-1}) at 1500–2000 m depth in the Equatorial domain (Figures 3, 4, 5, and 6). Eastward deflection of the southward flowing DWBC along and just south of the equator has been observed in the NADW domain [*Weiss et al.*, 1985; *Richardson and Schmitz*, 1994; *Rhein et al.*, 1995; *Andrié*, 1996; *Mercier and Arhan*, 1997; *Arhan et al.*, 1998]. A uniform layer of $S > 34.9$, $pH > 7.97$, NTA < 2350 μmol kg^{-1} and $NC_T < 2200$ μmol kg^{-1} was observed below the core of UNADW, which correspond to the deeper branches of NADW. A bend in the θ-S at ~2°C (not shown), coined as the Two-Degree Discontinuity (TDD) by *Broecker et al.* [1976], constitutes the lower limit of depth of the NADW. This limit is at ~4000 m on the northern end of A14, indicating that the deepest branches of NADW cross the Mid-Atlantic Ridge (MAR) through the Romanche Fracture Zone to enter the Eastern South Atlantic [*Friedrichs et al.*, 1994; *Mercier and Morin*, 1997].

[28] An isolate NTA minimum (<2330 μmol kg^{-1}) at 1400–1700 m near 13°S (Figure 5) depicts the presence of a zonal jet transporting UNADW. According to *Stramma and England* [1999], NADW flows westward at ~15°S as a result of recirculation at the eastern flank of the MAR UNADW and UCPW encountered at 23°S, where they form a marked front that is easily observed in the distributions of

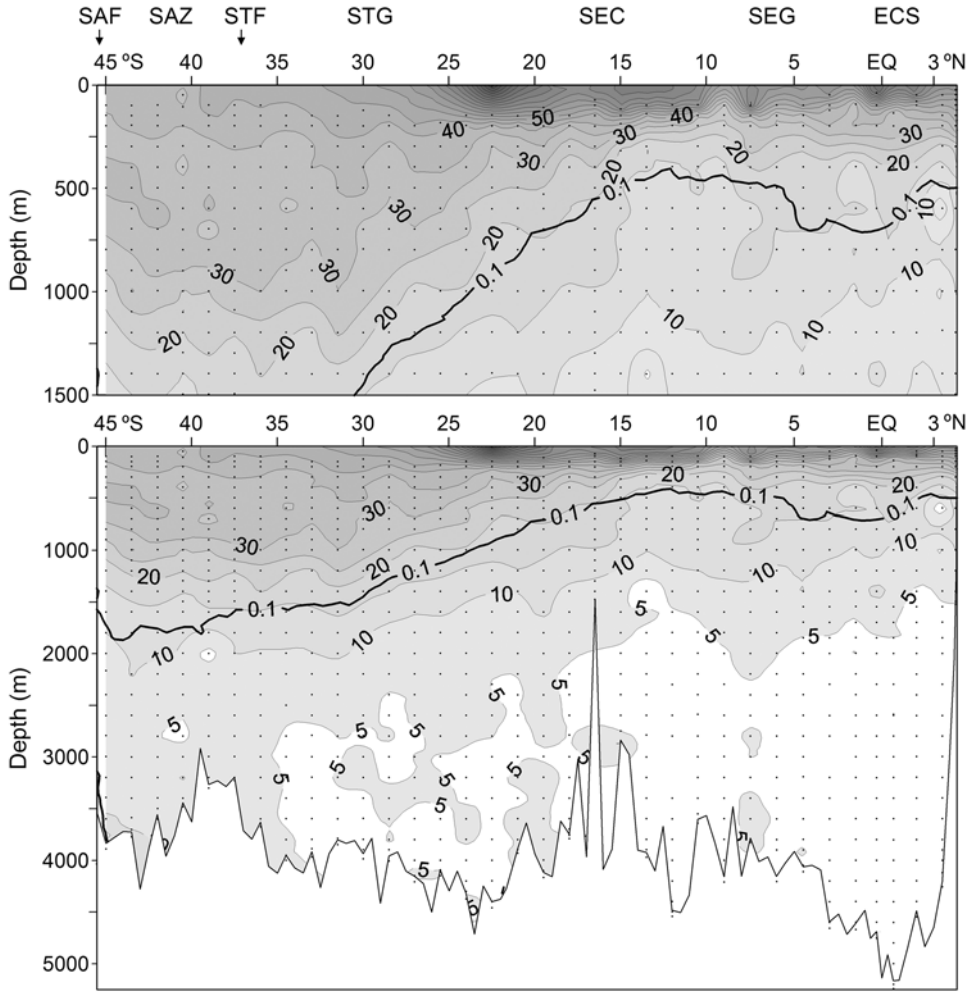

Figure 10. Vertical distribution of anthropogenic carbon (μmol kg^{-1}) along line A14. Solid line represents CFC11 isoline of 0.1 pmol kg^{-1}.

all the study properties (Figures 3, 4, 5, 6, and 10). As a consequence, NADW flows to the eastern basin through the Rio de Janeiro (22°S) and the Río Grande (26°S) Fracture Zones of the MAR [*Mercier et al.*, 2000], and is deflected eastwards to meet a zonal jet that *Warren and Speer* [1991] called the "Namib Col Current" near 22°S in the Angola Basin. The existence of an eastward flow near 25°S centered at 2000 m, which transports NADW from the western South Atlantic, was first suggested by *Reid* [1989] and corroborated by *Speer et al.* [1995]. Local maxima of salinity and pH and minima of NTA and NC_T at ~22°S in the UNADW domain (~1800 m) traced the "Namib Col Current" along A14. To the south of 23°S, the deeper branches of NADW can be observed, centered at 2400 m, by the distributions of the measured variables (Figures 3, 4, 5, 6, and 10).

[29] Antarctic Bottom Water (AABW) along A14 consisted exclusively of Lower Circumpolar Water (LCPW) since the >46.04 σ_4 characteristic density of Weddell Sea Deep Water (WDSW) was not observed. AABW can be distinguished in the southernmost side of the section by low pH_{15} (7.881–7.915) and high NTA (2370–2380 μmol kg^{-1}) and NC_T (2260–2270μmol kg^{-1}) values in the bottom layer, spreading north to 36°S. At this point, the Walvis ridge limits the northward extension of AABW. Minor volumes of this water mass were observed in abyssal depths (>4000 m, <2°C) at the equator, which enter from the western basins through the Romanche Fracture zone and can be traced by high NTA (2355–2360 μmol kg^{-1}) and NC_T (2210–2215 μmol kg^{-1}) concentrations.

3.2. Anthropogenic CO_2

[30] The method used for calculating anthropogenic carbon (C_{ANT}) is based on a modification of the back-calculation technique proposed by *Brewer* [1978] and *Chen and Millero* [1979], further modified by *Gruber et al.* [1996] and improved by *Pérez et al.* [2002]. In this technique, correction of the effect of organic carbon oxidation and $CaCO_3$ dissolution processes on the distribution of C_T allows the determination of the initial CO_2 (C_T^0) of different water masses in source regions. In addition, assuming that dissolved oxygen and CO_2 are close to equilibrium (or with the same disequilibrium) with the atmosphere during waters mass formation, C_T^0 has progressively increased since the preindustrial era. Conversely, TA^0 is not significantly affected by the entry of anthropogenic CO_2 because in surface waters that are $CaCO_3$ supersaturated, $CaCO_3$ dissolution due to progressive acidification is negligible [*Chen*

and Millero, 1979; *Poisson and Chen*, 1987; *Gruber et al.*, 1996]. The total amount of anthropogenic CO_2 trapped in any parcel of water (C_{ANT}) according to *Ríos et al.* [2001] and *Pérez et al.* [2002] is calculated from C_T, TA and dissolved oxygen measured at the sea:

$$C_{ANT} = C_T - AOU/R_C - 1/2 \cdot (TA - TA^0 + AOU/R_N) - C^0_{T278}, \quad (4)$$

where AOU/R_C is the C_T increase by organic matter oxidation. Apparent Oxygen Utilization (AOU) is calculated with the oxygen saturation equation of *Benson and Krause* [*UNESCO*, 1986]. R_C is a stoichiometric coefficient ($=-\Delta O_2/\Delta C$). Additionally, $1/2\cdot(\Delta TA + AOU/R_N)$ is the C_T change due to $CaCO_3$ dissolution in deep ocean waters [*Broecker and Peng*, 1982], where ΔTA is the total alkalinity change from the initial value during water mass formation (TA^0), and R_N is a second stoichiometric coefficient ($=-\Delta O_2/\Delta N$). For open ocean waters below 400 m $R_C = 1.45$ and $R_N = 10.6$ [*Anderson and Sarmiento*, 1994]. TA^0 stands for preformed alkalinity and was calculated using the A14 database, with an error of the estimation of 4.4 μmol kg^{-1}, from salinity and "PO" for the layer between 50 and 200 m, as the best approximation to the winter mixed layer, using the empirical equation obtained: $TA^0 = 336.86 + 56.23\cdot S + 0.0200\cdot$'PO' ($r^2 = 0.97$, $n = 116$, $p < 0.001$) where "PO" $= O_2 + R_P\cdot PO_4$. R_P is a stoichiometric coefficient ($= -\Delta O_2/\Delta P$) with a constant value of 170 molO_2/molP [*Anderson and Sarmiento*, 1994]. C^0_{T278} is the initial C_T of any water mass in the preindustrial era, which can be calculated from time-independent TA^0 and the atmospheric pCO_2 level at that time and water vapor pressure [*Pérez et al.*, 2002], where $pCO_2 = xCO_2{}^0\cdot$(Patm-vapor pressure) according to *U.S. Department of Energy* [1994]. The mole fraction of CO_2 in the preindustrial atmosphere ($xCO_2{}^0$) was 278.2 ppm [*Neftel et al.*, 1994; *Sarmiento et al.*, 1995]. The method to estimate C_{ANT} is subject to a number of uncertainties. Using an error propagation analysis for C_{ANT} as given by *Gruber et al.* [1996] and *Sabine et al.* [1999], the maximum error associated with the C_{ANT} calculation was ±5.6 μmol·kg^{-1}.

[31] The distribution of C_{ANT} along A14 is shown in Figure 10. The 0.1 pmol kg^{-1} CFC11 isoline, corresponding roughly to an apparent age of 37–39 years, is traced along the C_{ANT} isoline of 15 μmol kg^{-1}. In general, C_{ANT} was a maximum in the upper 200 m, with the highest values (45–75 μmol kg^{-1}) to the north of 23°S (Figure 10). Minimum penetration of C_{ANT} was observed in the equatorial zone, where the C_{ANT} isoline of 15 μmol kg^{-1} was situated at ~400 m due to the upwelling of old waters. The reduced C_{ANT} penetration extended to 15°S, at the subequatorial-subtropical transition. Further south, within the STG, large-scale downwelling produced a relative sink of the C_{ANT} rich upper waters that contribute to the penetration of new water volumes which were ventilated to the south of the STF. Concentrations >10 μmol kg^{-1} were found above a depth of ~2000 m in the STG, whereas south of the STF the isoline of 10 μmol kg^{-1} extended to ~2200 m. The invasion of C_{ANT} is remarkable south of 23°S, especially south of the STF where the isoline of 5 μmol kg^{-1} reaches the bottom,

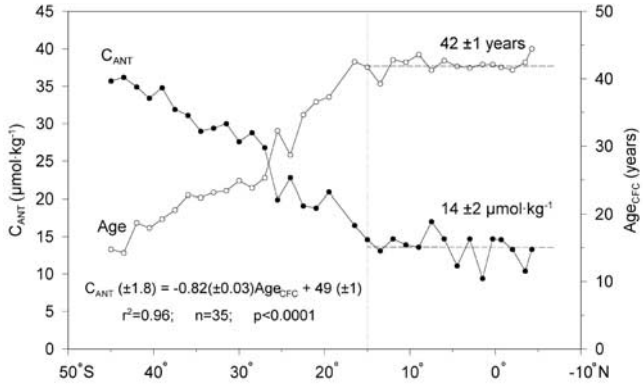

Figure 11. Meridional evolution of anthropogenic carbon (C_{ANT}) and "apparent age" calculated through CFC11 (Age_{CFC}) in the AAIW salinity minimum along A14. The linear regression between C_{ANT} and Age_{CFC} is reported.

corresponding with the penetration of AABW. It is interesting to note that the penetration of C_{ANT} at the NADW domain in the Eastern South Atlantic had already begun at the core of eastward flowing UNADW centered at ~1400 m at the equator.

[32] The distribution of C_{ANT} along A14 (Figure 10), was similar to that described by *Chen* [1982] (GEOSECS 1973), *Gruber* [1998] (SAVE 1989) east of A14, and *Wanninkhof et al.* [1999] (NOAA/OACES 1991) west of A14, although with some remarkable differences. In general, the C_{ANT} penetration was deeper during A14 than found by these authors, mainly due to the time elapsed among different database used in the C_{ANT} estimates. In addition, the C_{ANT} estimates can vary depending on the method used [*Wanninkhof et al.*, 1999].

[33] AAIW in the Subantarctic Zone (south of 36–37°S) appears as a thick layer of salinity <34.2 (Figure 3), which transports the high C_{ANT} concentrations (>30 μmol kg^{-1}) acquired south of the SAF to the interior of the South Atlantic. Figure 11 shows the meridional evolution of C_{ANT} along the AAIW salinity minimum during A14. Maximum C_{ANT} values of 36 μmol kg^{-1} were observed at the southern end of the section (45°30′S) and decreased northward 15°S. North of 15°S, C_{ANT} became constant at 14 ± 2 μmol kg^{-1}. CFC11 exhibited the same trend as C_{ANT} along the AAIW salinity minimum, as suggested by the corresponding linear regression ($r^2 = 0.88$, $n = 35$, $p < 0.0001$):

$$C_{ANT}(\pm 2.9) = 15.2(\pm 0.6) + 7.5(\pm 0.5)\ \text{CFC11}. \quad (5)$$

[34] *Warner and Weiss* [1992] found similar CFC11 and CFC12 evolutions at the AAIW 27.2 isopycnal surface along the prime meridian during the Ajax expeditions (1983–1984). In their study the concentrations of both CFCs became constant at 20°S instead of at 15°S, which we observed 10 years later.

[35] CFC concentrations supply information on time scales of oceanic processes such as advection and mixing. Equilibration with the overlying atmosphere at the time of water mass formation is usually invoked during the estimation of water mass ages by means of CFC concentrations [*Warner and Weiss*, 1992]. The "apparent age" (Age_{CFC}) of

AAIW at the salinity minimum can be calculated converting the measured CFC11concentrations into CFC-11 partial pressures (pCFC11) [*Doney and Bullister*, 1992]:

$$\mathrm{pCFC-11} = [\mathrm{CFC11}] \cdot \mathrm{F}^{-1}, \quad (6)$$

where F is the solubility of CFC11, a function of potential temperature and salinity given by *Warner and Weiss* [1985]. Age_{CFC} is then obtained matching the calculated pCFC11 with the atmospheric pCFC11 record. Reconstructed CFC11 annual mean dry air mole fractions in the Southern Hemisphere were used [*Walker et al.*, 2000]. The course of Age_{CFC} at the AAIW salinity minimum along A14 referred to 1995 (Figure 11) is a mirror image of C_{ANT}. AAIW at 45°30'S was ~15 years old and became older as it evolved northwards. North of 15°S, Age_{CFC} was constant at 42 ± 1 year. There was a very good correlation between C_{ANT} and Age_{CFC} ($r^2 = 0.96$, n = 35, $p < 0.001$).

[36] According to this regression, the annual rate of C_{ANT} entry in the ocean via AAIW is 0.82 μmol kg^{-1} y^{-1}. This rate is in very good agreement with the annual rate of 0.80 μmol kg^{-1} y^{-1} estimated from the equilibrium between the upper mixed layer and the average atmospheric xCO_2 increase, according to *Keeling et al.* [1995]. In order to check the age of the AAIW salinity minimum at 45°S (C_{ANT} = 36 μmol kg^{-1} and Age_{CFC} = 15 years) a back calculation was performed. Calculated C_T^0 in the preindustrial time (xCO_2 = 278 ppm) and in 1980 (xCO_2 = 336 ppm) [*Keeling et al.*, 1995], 15 years before A14, were 2069 μmol kg^{-1} and 2100 μmol kg^{-1}, respectively. Therefore the net anthropogenic carbon uptake was 31 μmol kg^{-1} indicating that Age_{CFC} is comparable with the proper age of the water mass in this case. North of 15°S the CFC11 signal was below the detection limit. Consequently, we can only suggest that the AAIW was >42 years old in this zone.

[37] Similar C_{ANT} and Age_{CFC} calculations were performed for the overlying SACW 13°C isotherm along A14 (not shown). The average C_{ANT} entry along this isotherm was 33 ± 3 μmol kg^{-1}. The transition at 15°S separates the 22 ± 1 years old (Age_{CFC}) subequatorial SACW to the north from the 10 ± 1 years old subtropical SACW to the south, with C_{ANT} entries of 32 ± 4 and 34 ± 2 μmol kg^{-1}, respectively. The apparent age difference between the subtropical and subequatorial SACW branches (12 ± 2 years) exceeds the residence time of SACW in the SEG estimated by *Gordon and Bosley* [1991]. This indicates the time that subtropical SACW spends to arrive at the SEG through the SEC and then the ECS.

[38] Regarding the old and poorly ventilated UCPW just below the AAIW domain, the meridional evolution of C_{ANT} and Age_{CFC} have been examined along the core of maximum NTA (Figure 5). Constant C_{ANT} of 17 ± 2 and 13 ± 1.6 μmol kg^{-1} were obtained south and north of 15°S, respectively. The corresponding Age_{CFC} were 38 ± 5 and >45 ± 2 years. The youngest UCPW (33 ± 1.4 years) appeared south of the STF. The slight C_{ANT} penetration into the domain of the UNADW although coincident with the uncertainty (5.9 ± 2.0 μmol kg^{-1}), showed a systematic signal. This signal was also visible on the transect NOAA/OACES [*Wanninkhof et al.*, 1999]. The penetration below 2500 m, south of 23°S, with AABW influence, showed an average C_{ANT} of 5.7 ± 2.0 μmol kg^{-1}, while

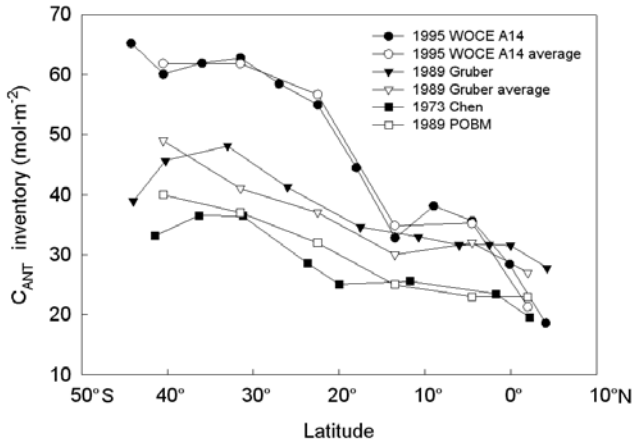

Figure 12. Meridional evolution of C_{ANT} inventories of WOCE A14 (black dots), averaged WOCE A14 (open dots), Gruber (black triangles down), averaged Gruber (open triangles down), Chen (black squares), and POBM (open squares).

north of 23°S in the domain of the aged middle and deep NADW, the C_{ANT} signal (2.6 ± 2.4 μmol kg^{-1}) is not significant. Since the standard deviation of C_{ANT} for this old water is 2.4 μmol kg^{-1}, the uncertainty of 5.6 μmol kg^{-1} obtained by calculation of error propagation is coherent.

[39] In order to estimate the inventory of anthropogenic carbon along A14, calculated C_{ANT} values were depth integrated from the surface (except the shallowest waters with AOU < 0) to entire water column, erasing negative values. The average C_{ANT} inventory for the entire line A14 was 540 gC m^{-2}. Figure 12 provides the C_{ANT} specific inventory for the different zones intersected by A14. South of 15°S, the specific inventory is twice that north of 15°S so that nearly 70% of the C_{ANT} penetration occurred in the subantarctic and subtropical domains. A comparison of the C_{ANT} inventory by zonal bands between A14, *Chen* [1982], *Gruber* [1998] estimate for 1989, and *Sarmiento et al.* [1995] calculations with the Princeton Ocean Biogeochemistry Model (POBM) has been made (Figure 12). The C_{ANT} specific inventory for A14 (black dots) was binned (open dots) in the same latitude bands as *Gruber* [1998], represented by open triangles down, to facilitate the comparison. Inventory from *Gruber* [1998] was estimated from the zonal section of C_{ANT} of his Figure 10 and represented by black triangles down (Figure 12). The average inventory for 1989 obtained using a segment with the same range of latitude as the A14 line, was 440 gC m^{-2} that is in agreement with the average specific inventory (36 mol m^{-2}) taken from Table 4 of *Gruber* [1998]. In the same way we have estimated the inventory from *Chen* [1982], using the C_{ANT} vertical distribution of his Figure 4, obtaining an average inventory of 342 gC m^{-2} for 1973.

[40] The zonal distribution of our C_{ANT} specific inventory is higher than *Gruber*'s [1998] and *Chen*'s [1982] inventories, showing differences of 20 and 29 mol m^{-2}, respectively, south of 15°S. The differences are lower north of 15°S (5 and 12 mol m^{-2}, respectively). In the equatorial zone our C_{ANT} inventories are slightly lower (5 mol m^{-2}) than Gruber's and slightly higher (2 mol m^{-2}) than Chen's

estimations. In the equatorial zone the ocean could be acting as a source due to the upwelling in this zone, favoring that water loaded with C_{ANT} reaches the surface water. Also, this decrease in the C_{ANT} inventories in the equatorial zone could be affected by the differences in station locations with regard to the coast.

[41] The average C_{ANT} specific inventory (45 mol m^{-2}) for A14 is higher than the estimate by *Gruber* and *Chen* in 9 and 16 mol m^{-2}, respectively. Our inventory is also higher in 15 mol m^{-2} than the POBM model for the South Atlantic Ocean for 1989. The zonal distribution of the POBM corresponds very well with the *Chen* [1982] estimate for 1973. Taking into account these inventory differences from our data, increase rates of 0.73 mol m^{-2} y^{-1} with regard to *Chen* [1982] and 1.5 mol m^{-2} y^{-1} to *Gruber* [1998] were obtained. The inventory difference between *Gruber* [1998] and *Chen* [1982] of 7 mol m^{-2}, results in an increase rate of 0.44 mol m^{-2} y^{-1}.

[42] Considering the annual rate of C_{ANT} entry in the ocean via AAIW is 0.82 μmol m^{-2} y^{-1} and the maximum depth penetration of this water reaches about 800 m, the atmospheric input of C_{ANT} is 0.67 mol m^{-2} y^{-1} that agrees with the increase rate estimated between A14 and *Chen* [1982] inventories for the period 1973–1995. Conversely, the increase rates calculated from *Gruber* [1998] inventory with regard to *Chen* [1982] and W14, for the periods 1973–1989 and 1989–1995, respectively, does not show this agreement. Although it can be expected that the penetration would increase in recent years, it seems to be very high for the period 1989–1995 and rather low between 1973 and 1989.

4. Conclusions

[43] Accurate estimation of the CO_2 anthropogenic entry in the oceans requires an accurate, precise and consistent database. The accuracy was tested by means of CRMs and the precision by duplicate analyses. The consistency was assessed by in situ measurements of three CO_2 system parameters. Knowledge of the dependence of CO_2 system parameter distributions on water masses ventilation, circulation, and mixing patterns is needed to better understand how the anthropogenic CO_2 penetration is produced. On the basis of these considerations we can summarize the following conclusions regarding the meridional evolution of measured and derived CO_2 system parameters along line A14:

[44] 1. Simultaneous measurements of three CO_2 system variables, the systematic use of CO_2 certified reference materials, and the collection of samples for comparison with manometric C_T measurements at SIO provided a means to test the accuracy and consistency of our shipboard measurements. CO_2 data produced during A14 were quite reliable to use for estimation of the potential of the Eastern South Atlantic as an anthropogenic CO_2 trap.

[45] 2. The power of CO_2 system parameters as tracers of the ventilation, circulation, and mixing patterns of water masses in the Eastern South Atlantic has been explored. The subtropical and subequatorial branches of SACW have been characterized by the pH_{15}, NTA, and NC_T meridional evolution along the 13°C isotherm. The CPW can be traced by the conspicuous NTA maximum. Maximum pH_{15} and minimum NTA and NC_T values allows characterization of NADW, marking important zonal flows in the UNADW domains at the equator, 13°S and 22°S. CO_2 system variables also characterized AABW on the northern (Romanche Fracture Zone) and southern (south of the Walvis Ridge) sides of line A14.

[46] 3. About 70% of the anthropogenic CO_2 accumulated by the Eastern South Atlantic along A14 during the industrial era occurred in the subantarctic and subtropical domains, where penetration depths were maximum. Extreme values of C_{ANT} are observed in the AAIW domain, being maximum in the relatively young AAIW of the subantarctic zone and minimum in the very old AAIW of the subequatorial gyre. The annual rate of C_{ANT} incorporation by AAIW is 0.82 μmol kg^{-1} y^{-1}, in agreement with the annual rate (0.8 μmol kg^{-1} y^{-1}) estimated from the equilibrium between the upper mixed layer and the atmospheric pCO_2 increase in the section.

[47] **Acknowledgments.** We would like to thank the master, officers, and crew of R/V L'Atalante and all the participants on the cruise CITHER-3. We are very grateful to T. Rellán for pH and alkalinity measurements and preparation of figures, A. Billant and J.P. Gouillou in charge of the CTD, M.J. Messias for CFC measurements, M.J. Pazó for nutrients and chlorophyll determinations, and Melchor González-Dávila for providing pH_{SWS} measured on CRM batch 24. Special thanks to M. Arhan (coordinator of the WOCE-France program CITHER) and H. Mercier (chief scientist of cruise CITHER 3). This work was supported by the Spanish CICYT (grant ANT94-1168-E) and IFREMER (University contract 94 1430 087).

References

Álvarez-Salgado, X. A., F. Fraga, and F. F. Pérez, Determination of nutrients salts by automatic methods both in sea and brackish water: The phosphate blank, *Mar. Chem.*, *39*, 311–319, 1992.

Anderson, L. A., and J. L. Sarmiento, Redfield ratios of remineralization determined by nutrient data analysis, *Global Biogeochem. Cycles*, *8*, 65–80, 1994.

Andrié, C., Chlorofluoromethanes in the Deep Equatorial Atlantic revisited, in *The South Atlantic: Present and Past Circulation*, edited by G. Wefer et al., pp. 273–288, Springer-Verlag, New York, 1996.

Andrié, C., C. Oudot, C. Genthon, and L. Merlivat, CO_2 fluxes in the Tropical Atlantic during FOCAL cruises, *J. Geophys. Res.*, *91*, 11,741–11,755, 1986.

Andrié, C., J.-F. Ternon, M.-J. Messias, L. Mémery, and B. Bourlès, Chlorofluoromethanes distributions in the deep equatorial Atlantic during January–March 1993, *Deep Sea Res.*, *45*, 903–930, 1998.

Arhan, M., H. Mercier, B. Bourlès, and Y. Gouriou, Hydrographic sections across the Atlantic at 7°30N and 4°30S, *Deep Sea Res., Part I*, *45*, 829–872, 1998.

Arhan, M., H. Mercier, and J. Lutjeharms, The disparate evolution of the three Agulhas rings in the South Atlantic Ocean, *J. Geophys. Res.*, *104*, 20,987–21,005, 1999.

Bakker, D. C. E., H. J. W. de Baar, and E. de Jong, The dependence on temperature and salinity of dissolved inorganic carbon in east Atlantic surface waters, *Mar. Chem.*, *65*, 263–280, 1999.

Boebel, O., C. Schmid, and W. Zenk, Flow and recirculation of Antartic Intermediate Water across the Rio Grande Rise, *J. Geophys. Res.*, *102*, 20,967–20,986, 1997.

Brea, S., Hidrografía del Sureste Atlántico, Sección WOCE A14 (4°N–46°S), BSC thesis, 71 pp., Univ. de Vigo, Vigo, Spain, 1998.

Brewer, P., Direct observation of the oceanic CO2 increase, *Geophys. Res. Lett.*, *5*, 997–1000, 1978.

Broecker, W. S., and T.-H. Peng, *Tracers in the Sea*, 690 pp., Lamont-Doherty Earth Observatory, Palisades, N.Y., 1982.

Broecker, W. S., T. Takahashi, and Y. H. Li, Hydrography of the central Atlantic–I. The two-degree discontinuity, *Deep Sea Res.*, *23*, 1083–1104, 1976.

Bullister, J. L., and R. F. Weiss, Determination of CCl_3F and CCl_2F_2 in seawater and air, *Deep Sea Res.*, *35*, 839–853, 1988.

Chen, C. T., On the distribution of anthropogenic CO_2 in the Atlantic and Southern Oceans, *Deep Sea Res.*, *29*, 563–580, 1982.

Chen, C. T., and F. J. Millero, Gradual increase of oceanic carbon dioxide, *Nature*, *277*, 205–206, 1979.

Clayton, T. D., R. H. Byrne, J. A. Breland, R. A. Feely, F. J. Millero, D. M. Campbell, P. P. Murphy, and M. F. Lamb, The role of pH measurements in modern oceanic CO_2-system characterizations: Precision and thermodynamic consistency, *Deep Sea Res., Part II*, *42*, 411–429, 1995.

Dickson, A. G., An exact definition of total alkalinity and procedure for the estimation of alkalinity and total inorganic carbon from titration data, *Deep Sea Res.*, *28*, 609–623, 1981.

Dickson, A. G., and J. P. Riley, The estimation of the acid dissociation constants in seawater media from potentiometric titrations with strong base. I. The ionic product of water *Kw*, *Mar. Chem.*, *7*, 89–99, 1979.

Doney, S. C., and J. L. Bullister, A chlorofluorocarbon section in the eastern North Atlantic, *Deep Sea Res., Part I*, *39*, 1857–1883, 1992.

Edmond, J. M., and J. M. Gieskes, On the calculation of the degree of saturation of sea water with respect to calcium carbonate under in situ conditions, *Geochim. Cosmochim. Acta*, *34*, 1261–1291, 1970.

Friedrichs, M. A. M., M. S. McCartney, and M. M. Hall, Hemispheric asymmetry of deep water transport modes in the Atlantic, *J. Geophys. Res.*, *99*, 25,165–25,179, 1994.

Gordon, A. L., and K. T. Bosley, Cyclonic gyre in the Tropical South Atlantic, *Deep Sea Res.*, *38*, S323–S343, 1991.

Groupe CITHER-3, Recueil de Données, Campagne CITHER 3, N/O L'Atalante (11 Janvier–2 Avril 1995), vol. 2, CTD-O2, *Rapport Interne LPO 96-05*, 532 pp., IFREMER/Centre de Brest, Plouzané, France, 1996.

Groupe CITHER-3, Recueil de Données, Campagne CITHER 3, N/O L'Atalante (11 Janvier–2 Avril 1995), vol. 3, Traceurs Géochimiques. *Rapport Interne LPO 98-03*, 586 pp., IFREMER/Centre de Brest, Plouzané, France, 1998.

Gruber, N., Anthropogenic CO_2 in the Atlantic Ocean, *Global Biogeochem. Cycles*, *12*, 165–191, 1998.

Gruber, N., J. L. Sarmiento, and T. F. Stocker, An improved method for detecting anthropogenic CO_2 in the oceans, *Global Biogeochem. Cycles*, *10*, 809–837, 1996.

Hansen, H. P., and K. Grasshoff, Automated chemical analysis, in *Methods of Seawater Analysis*, edited by K. Grasshoff, M. Ehrhardt, and K. Kremlig, 419 pp., Springer-Verlag, New York, 1983.

Johnson, K. M., P. J. L. Williams, and L. Brändström, Coulometric TCO_2 analysis for marine studies: Automation and calibration, *Mar. Chem.*, *21*, 117–133, 1987.

Johnson, K. M., K. D. Wills, D. B. Butler, W. K. Johnson, and C. S. Wong, Coulometric total carbon dioxide analysis for marine studies: Maximizing the performance of an automated gas extraction system and coulometric detector, *Mar. Chem.*, *17*, 1–21, 1993.

Johnson, K. M., A. Körtzinger, L. Mintrop, J. C. Duinker, and D. W. R. Wallace, Coulometric total carbon dioxide analysis for marine studies: Measurements and internal consistency of underway TCO_2 concentrations, *Mar. Chem.*, *67*, 123–144, 1999.

Joyce, T., and C. Corry, Requirements for WOCE Hydrographic Programme data reporting, *WHP Off. Rep. 90-1 WOCE Rep. 67/91*, 144 pp., Natl. Sci. Found., Woods Hole, Mass., 1994.

Keeling, C. D., T. P. Whorf, M. Wahlen, and J. van der Plicht, Interannual extremes in the rate of rise of atmospheric carbon dioxide since 1980, *Nature*, *375*, 666–670, 1995.

Larqué, L., K. Maamaatuaiahutapu, and V. Garçon, On the intermediate and deep water flows in the South Atlantic Ocean, *J. Geophys. Res.*, *102*, 12,425–12,440, 1997.

Lee, K., F. J. Millero, and R. Wanninkhof, The carbon dioxide system in the Atlantic Ocean, *J. Geophys. Res.*, *102*, 15,693–15,707, 1997.

Lefèvre, N., G. Moore, J. Aiken, A. Watson, D. Cooper, and R. Ling, Variability of pCO_2 in the tropical Atlantic in 1995, *J. Geophys. Res.*, *103*, 5623–5634, 1998.

Lyman, J., Buffer mechanism of seawater, Ph.D. thesis, 196 pp., Univ. of California, Los Angeles, Los Angeles, Calif., 1956.

McCartney, M. S., Crossing of the equator by the deep western boundary current in the western Atlantic Ocean, *J. Phys. Oceanogr.*, *23*, 1953–1974, 1993.

McElligott, S., R. H. Byrne, K. Lee, R. Wanninkhof, F. J. Millero, and R. A. Feely, Discrete water column measurements of CO_2 fugacity and pH_T in seawater: A comparison of direct measurements and thermodynamic calculations, *Mar. Chem.*, *60*, 63–73, 1998.

Mehrbach, C., C. H. Culberson, J. E. Hawley, and R. M. Pytkowicz, Measurements of the apparent dissociation constant of carbonic acid in seawater at atmospheric pressure, *Limnol. Ocean*, *8*, 897–907, 1973.

Mémery, L., M. Arhan, X. A. Alvarez-Salgado, M.-J. Messias, H. Mercier, G. C. Castro, and A. F. Ríos, The water masses along the western boundary of the south and equatorial Atlantic, *Progr. Oceanogr.*, *47*, 69–98, 2000.

Mercier, H., and M. Arhan, Two meridional hydrographic sections in the eastern South Atlantic Ocean (WHP lines A13 and A14), *Intl. WOCE Newsl.*, *28*, 28–30, 1997.

Mercier, H., and P. Morin, Hydrography of the Romanche and Chain Fracture Zones, *J. Geophys. Res.*, *102*, 10,373–10,389, 1997.

Mercier, H., G. L. Weatherly, and M. Arhan, Bottom water throughflows at the Río de Janeiro and Río Grande Fracture Zones, *Geophys. Res. Lett.*, *27*, 1503–1506, 2000.

Millero, F. J., Thermodynamics of the carbon dioxide system in the oceans, *Geochim. Cosmochim. Acta*, *59*, 661–677, 1995.

Millero, F. J., R. H. Byrne, R. Wanninkhof, R. Feely, T. D. Clayton, P. Murphy, and M. F. Lamb, The internal consistency of CO_2 measurements in the equatorial Pacific, *Mar. Chem.*, *44*, 269–280, 1993.

Mouriño, C., and F. Fraga, Determinación de nitratos en agua de mar, *Invest. Pesq.*, *49*, 81–96, 1985.

Neftel, A., H. Friedli, E. Moor, H. Lötscher, H. Oeschger, U. Siegenthaler, and B. Stauffer, Historical CO_2 record from the Siple station ice core, in *Trends '93: A Compendium of Data on Global Change*, *Rep. ORNL/CDIAC-65*, pp. 11–14, edited by T. Boden et al., Carbon Dioxide Inf. Anal. Cent., Oak Ridge Nath. Lab., Oak Ridge, Tenn., 1994.

Oudot, C., and C. Andrié, Short term changes in the partial pressure of CO_2 in the eastern tropical Atlantic surface seawater and in atmospheric CO_2 mole fraction, *Tellus, Ser. B*, *41*, 537–553, 1989.

Oudot, C., C. Andrié, and Y. Montel, Evolution du CO_2 océanique et atmosphérique sur la période 1982–1984 dans l'Atlantique tropical, *Deep Sea. Res.*, *34*, 1107–1137, 1987.

Oudot, C., P. Morin, F. Baurand, M. Wafar, and P. Le Corre, Northern and southern water masses in the equatorial Atlantic: Distribution of nutrients in the WOCE A6 and A7 lines, *Deep Sea Res., Part I*, *45*, 873–902, 1998.

Pérez, F. F., and F. Fraga, The pH measurements in seawater on NBS scale, *Mar. Chem.*, *21*, 315–327, 1987a.

Pérez, F. F., and F. Fraga, A precise and rapid analytical procedure for alkalinity determination, *Mar. Chem.*, *21*, 169–182, 1987b.

Pérez, F. F., M. Álvarez, and A. F. Ríos, Improvements on the back-calculation technique for estimating anthropogenic CO_2, *Deep Sea Res., Part I*, *49*, 859–875, 2002.

Peterson, R. G., and L. Stramma, Upper-level circulation in the South Atlantic Ocean, *Prog. Oceanogr.*, *26*, 1–73, 1991.

Peterson, R. G., and T. Whitworth, The subantarctic and polar fronts in relation to deep water masses through the Southwestern Atlantic, *J. Geophys. Res.*, *94*, 10,817–10,838, 1989.

Poisson, A., and C. T. A. Chen, Why is there little anthropogenic CO_2 in the Antarctic Bottom water?, *Deep Sea Res.*, *34*, 1255–1275, 1987.

Reid, J. L., On the total geostrophic circulation of the South Atlantic Ocean: Flow patterns, tracers, and transports, *Prog. Oceanogr.*, *23*, 149–244, 1989.

Rhein, M., L. Stramma, and U. Send, The Atlantic deep western boundary current: Water masses and transports near the equator, *J. Geophys. Res.*, *100*, 2441–2457, 1995.

Richardson, P. L., and W. J. Schmitz, Deep cross-equatorial flow in the Atlantic measured with SOFAR floats, *J. Geophys. Res.*, *98*, 8371–8387, 1994.

Ríos, A. F., F. F. Pérez, and F. Fraga, Long-term (1977–1997) measurements of carbon dioxide in the Eastern North Atlantic: Evaluation of anthropogenic input, *Deep Sea Res., Part II*, *48*, 2227–2239, 2001.

Sarmiento, J. L., R. Murnane, and C. Le Quere, Air-sea CO_2 transfer and the carbon budget of the North Atlantic, *Phil. Trans. R. Soc. London*, *348*, 211–219, 1995.

Siedler, G., N. Zangenberg, R. Onkeb, and A. Morlière, Seasonal changes in the tropical Atlantic circulation: Observation and simulation of the Guinea Dome, *J. Geophys. Res.*, *97*, 703–715, 1992.

Smethie, W. M., T. Takahashi, and D. W. Chipmam, Gas exchange and CO_2 flux in the Tropical Atlantic Ocean determined from ^{222}Rn and pCO_2 measurements, *J. Geophys. Res.*, *90*, 7005–7022, 1985.

Speer, K. G., G. Siedler, and L. Talley, The namib col current, *Deep Sea Res., Part I*, *42*, 1933–1950, 1995.

Stramma, L., and M. England, On the water masses and mean circulation of the South Atlantic Ocean, *J. Geophys. Res.*, *104*, 20,863–20,883, 1999.

Takahashi, T., W. S. Broecker, and S. Langer, Redfield ratio based on chemical data from isopycnal surfaces, *J. Geophys. Res.*, *90*, 6907–6924, 1985.

Tsuchiya, M., L. D. Talley, and M. S. McCartney, Water-mass distributions in the western South Atlantic: A section from South Georgia Island (54°S) northward across the equator, *J. Mar. Res.*, *52*, 55–81, 1994.

UNESCO, Background papers and supporting data on the Practical Salinity Scale, 1978, *UNESCO Tech. Pap. Mar. Sci.*, *34*, 144 pp., 1981.

UNESCO, Progress on oceanographic tables and standards 1983–1986: Work and recommendations of the UNESCO/SCOR/ICES/IAPSO joint panel, *UNESCO Tech. Pap. Mar. Sci.*, *50*, 59 pp., 1986.

U.S. Department of Energy, Handbook of methods for the analysis of the various parameters of the carbon dioxide system in sea water, version 2.0, *USDOE SRGP-89-7A*, Washington, D.C., 1994.

Walker, S. J., R. F. Weiss, and P. K. Salameh, Reconstructed histories of the annual mean atmospheric mole fractions for the halocarbons CFC-11, CFC-12, CFC-113 and carbon tetrachloride, *J. Geophys. Res.*, *105*, 14,285–14,296, 2000.

Wanninkhof, R., S. C. Doney, T. H. Peng, J. L. Bullister, K. Lee, and R. A. Feely, Comparison of methods to determine the anthropogenic CO2 invasion into the Atlantic Ocean, *Tellus, Ser. B*, *51*, 511–530, 1999.

Warner, M. J., and R. F. Weiss, Solubilitys of chlorofluorocarbons 11 and 12 in water and seawater, *Deep Sea Res.*, *32*, 1485–1497, 1985.

Warner, M. J., and R. F. Weiss, Chlorofluoromethanes in south Atlantic Antarctic intermediate water, *Deep Sea Res., Part I*, *39*, 2053–2075, 1992.

Warren, B. A., and K. G. Speer, Deep circulation in the eastern South Atlantic Ocean, *Deep Sea Res., Part I*, *38*, S281–S322, 1991.

Watson, A. J., P. D. Nightingale, and D. J. Cooper, Modelling atmosphere-ocean CO_2 transfer, *Phil. Trans. R. Soc. London*, *348*, 125–132, 1995.

Weiss, R. F., Carbon dioxide in water and seawater: The solubility of a non-ideal gas, *Mar. Chem.*, *2*, 203–215, 1974.

Weiss, R. F., J. L. Bullister, R. H. Gammon, and M. J. Warner, Atmospheric chlorofluoromethanes in the deep equatorial Atlantic, *Nature*, *314*, 608–610, 1985.

Wüst, G., Die sratosphäre, *Wiss. Ergeb. Dtsch. Atl. Exped.*, *6*(1/2), 109–288, 1935.

Yentsch, C. S., and D. W. Menzel, A method for the determination of phytoplankton chlorophyll and pheophytin by fluorescence, *Deep Sea Res.*, *10*, 221–231, 1963.

X. A. Álvarez-Salgado, F. F. Pérez, and A. F. Ríos, CSIC, Instituto de Investigaciones Marinas, Eduardo Cabello 6, 36208-Vigo, Spain. (xsalgado@iim.csic.es; fiz@iim.csic.es; aida@iim.csic.es)

J. Arístegui, Universidad de las Palmas de Gran Canaria, Edificio de Ciencias Básicas, Campus Universitario Tafira, 35017 Las Palmas de Gran Canaria, Spain. (jaristegui@dbil.ulpgc.es)

L. S. Bingler, Pacific Northwest National Laboratory, Battelle Marine Sciences Laboratory, 1529 W. Sequim Bay Road, Sequim, WA 98382, USA. (l.bingler@pnl.gov)

L. Mémery, Laboratoire d'Océanographie Dynamique et Climatologie, Institut Pierre Simon Laplace, CNRS-IRD-UPMC, Case 100, 4 Place Jussieu, 75252, Paris Cedex 05, France. (Laurent.Memery@ipsl.jussieu.fr)